Evolution of X-ray activity of $1 - 3\ M_\odot$ late-type stars in early post-main-sequence phases

Nicola Pizzolato, Antonio Maggio, and Salvatore Sciortino

Istituto e Osservatorio Astronomico di Palermo, Italy

Abstract. We present preliminary results on the variation of coronal X-ray emission during early post-main-sequence phases, for a sample of 83 late-type stars (D < 100 pc), with estimated masses in the range $1 - 3\ M_\odot$ using HIPPARCOS parallaxes and recent evolutionary tracks (Schaller et al. 1992). These stars were observed with the ROSAT/PSPC; source detection and evaluation of X-ray fluxes (or upper limits) were achieved with the wavelet transform algorithm of Damiani et al. (1997). The aim of this work is to study the evolutionary history of X-ray activity in early post-main-sequence phases for stars with masses $1.5 < M/M_\odot < 3.0$ (inactive A-type stars on the main-sequence) with respect to lower mass solar-type stars. A trend of increasing X-ray luminosity with age for the higher mass stars is suggested by our ROSAT sample, and a similar evidence comes from two other independent samples: a sample of 24 stars observed with the *Einstein* satellite (Maggio et al. 1993), and a sample of 23 evolved stars extracted from the RIASS "coronathon" (Ayres et al. 1995). The results of the present study may help to test the expectation that magnetic dynamo activity depends on the evolutionary phase through several possible ingredients, and in particular the rotation history of coronal X-ray sources during the main-sequence lifetime, and mass-dependent changes of the stellar internal structure.

1. Sample Selection

Our ROSAT sample consists of 83 late type stars with $D < 100$ pc, using Hipparcos parallaxes, extracted from the Bright Star Catalogue (Hoffleit & Warren 1991) in the region of the H-R diagram with $0 < (B-V) < 1$ and $-5 < M_v < +5$ and above the main-sequence, and falling in ROSAT/PSPC images within $40'$ from the field center (either pointed or serendipitous observations). The ROSAT data were reprocessed with the Palermo-CfA pipeline (Mackie et al. 1996), where source detection and count rate (or upper limit) evaluation are performed with the wavelet transform algorithm of Damiani et al. (1997).

For comparison, we have also considered two other, independent star samples with the following characteristics:

- *Einstein* Observatory sample: 24 late type stars with $D < 50$ pc, mostly located between the evolutionary tracks for stars of $1 - 3\ M_\odot$, and observed with the *Einstein*/IPC, already studied by Maggio et al. (1993).

- RIASS sample: subsample of 23 evolved stars ($D < 50$ pc) extracted from the original sample of 91 *coronathon* candidates (Ayres et al. 1995) observed in the ROSAT-IUE All Sky Survey.

We have evaluated X-ray fluxes (or upper limits) for the stars in our ROSAT sample using the count rates, corrected for vignetting and contamination of nearby sources, and adopting a constant conversion factor of 6×10^{-12} erg cm^{-2} s^{-1} per count s^{-1}. In Fig. 1 we compare these X-ray fluxes with independent estimates, for the stars in common between our ROSAT sample and the *Einstein* or the RIASS samples. Although the stars in each sample have been observed in different epochs, the X-ray fluxes are in general agreement.

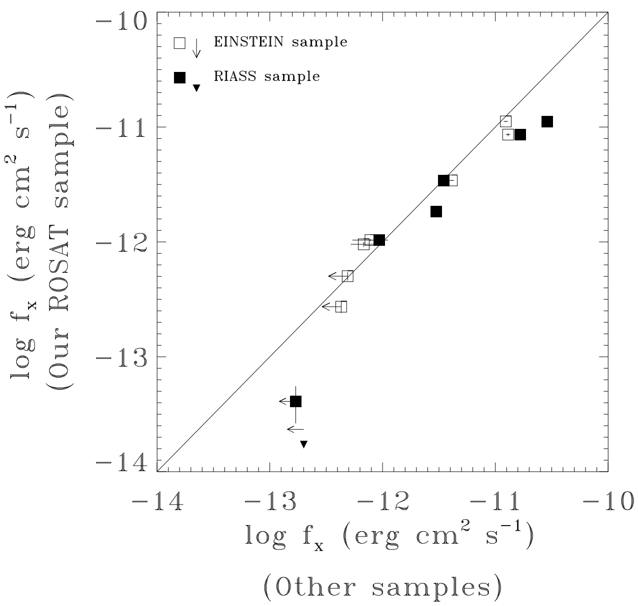

Figure 1. Comparison of X-ray fluxes (or upper limits) evaluated using the method of Damiani et al. (1997), based on wavelet transforms, and independent X-ray flux estimates for stars in common between our ROSAT sample and the *Einstein* or RIASS samples.

2. Determination of stellar evolutionary state and mass

In order to estimate masses and to assess the evolutionary states of the stars in our sample we have used and compared results based on two different sets of evolutionary tracks, with the following characteristics:

- VandenBerg evolutionary tracks (VandenBerg 1985):
  Y = 0.25, Z = 0.0169 and mixing length parameter $\alpha = 1.6$, Los Alamos opacities (Huebner et al. 1977), no overshooting, and model atmospheres of Kurucz (1979) used for the boundary conditions and for transposing the theoretical $T_{\rm eff}$-L diagram into a C-M diagram.

- Schaller et al. evolutionary tracks (Schaller et al. 1992):
  Y = 0.3, Z = 0.020 and mixing length parameter $\alpha = 1.6$, Rogers & Iglesias (1991) opacities and Kurucz (1991) opacities at low temperature, overshooting with $d_{over}/H_p = 0.2$, for stars with $M > 1.25$, and updated nuclear reaction rates and neutrino loss rates.

The observational C-M diagram for the ROSAT star sample was based on HIPPARCOS parallaxes and the stellar masses were computed via interpolation on the tracks, assuming all stars in first-crossing evolutionary phases. We have obtained consistent mass estimates, within 10%, using the two sets of tracks (Fig. 2). We have eventually adopted the masses based on the Schaller et al. evolutionary tracks for our study.

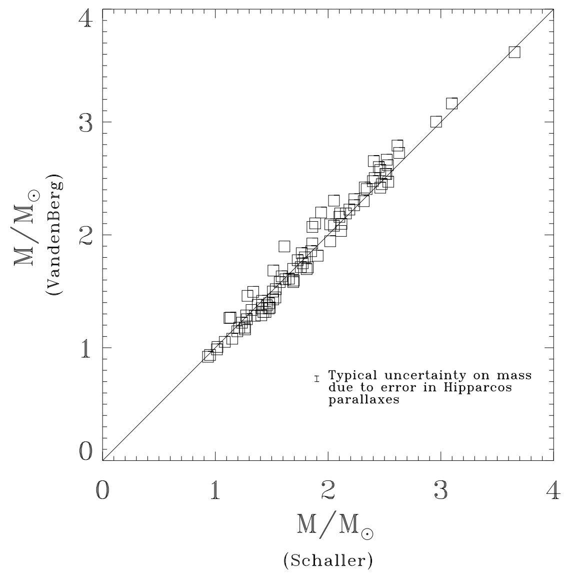

Figure 2. Comparison of $M/M_\odot$ obtained using the VandenBerg evolutionary tracks and the Schaller et al. evolutionary tracks, for our ROSAT star sample. Note the global agreement (within ~10%) between the two computations.

In order to check for possible observational biases we have studied the dependence of X-ray luminosity vs. stellar mass (Fig. 3) and vs. stellar distance in three mass ranges (Fig. 4). There is a tendency for the higher mass stars to be also more X-ray luminous (Fig. 3), but there exist also some high luminosity sources (log $L_x > 29.5$ erg s^{-1}) with relatively low masses ($M \leq 2M_\odot$). Fig. 4 shows that once we exclude stars with $D > 100$ pc we are left with a negligible dependence of L_x on star distance, so that our $D < 100$ pc sample is nearly free of distance-related observational biases.

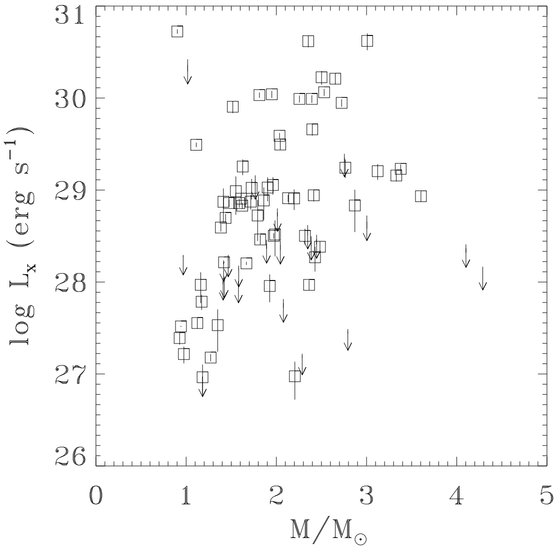

Figure 3. Scatter plot of X-ray luminosity (or upper limit) vs. stellar mass for the stars in the ROSAT sample with $D < 100$ pc.

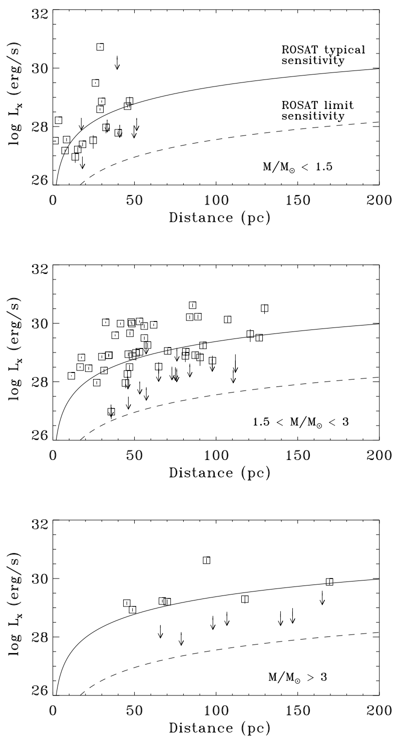

Figure 4. Scatter plots of X-ray luminosity (or upper limit) vs. star distance, in the three mass ranges indicated.

3. Results

We have selected three mass ranges for our ROSAT sample, in order to study separately stars with and without subphotospheric convective zones while on the main-sequence phase. In order to monitor the variation of X-ray activity during the evolution across the Hertzsprung gap, we study the distribution of X-ray luminosities vs. B-V color for the stars in each mass range (Fig. 5). In fact, since the evolutionary tracks are almost horizontal in the H-R diagram, during early post-main-sequence phases, the B-V color can be used as a proxy of the evolutionary age. Since in these phases the stellar radius increases appreciably, and the disk-integrated X-ray luminosity may depend on the available surface, we have considered also the distribution of surface X-ray fluxes vs. B-V color (Fig. 6), the former computed after evaluation of the stellar radius with the Barnes-Evans relation (Barnes et al. 1978).

Inspection of Fig. 5 and Fig. 6 suggests the following scenario:

- $M/M_\odot < 1.5$: these stars (F and G-type on the main-sequence) show relatively low X-ray emission levels ($27 < \log L_{\rm x} < 29$ and $3.5 < \log F_{\rm x} < 5.5$) in the $B-V$ range $0.4 \div 0.8$. The only two stars with $B-V > 0.8$ in our sample are instead intense X-ray emitters: they are GJ 732.1 (HD 175225) (plus), a suspected spectroscopic binary (Duquennoy & Mayor 1991), and HR 1099 (V 711 Tau) (asterisk), a well know RS CVn-type binary.

- $1.5 < M/M_\odot < 3.0$: these stars (A-type on the main-sequence) show on average an increasing X-ray emission level during the evolutionary phases across the Hertzsprung gap ($0.2 < B-V < 0.8$)($28 < \log L_{\rm x} < 30$ erg s^{-1} and $4 < \log F_{\rm x} < 6$ erg cm^{-2} s^{-1}). There are exceptions to this behavior, i.e. X-ray sources with $L_{\rm x}$ higher than average (the colors refer to the symbols in Fig. 5 and Fig. 6):

  - 13 Com, HD 107966 (plus), A-type, $v \sin i \sim 55$ km s^{-1}
  - HD 141851 (asterisk), A-type, interferometric binary, $v \sin i \sim 185$ km s^{-1}
  - 71 Tau, HD 28052 (open diamond), F0 V (SB), Hyades member, $v \sin i \sim 193$ km s^{-1}
  - HD 10308 (open triangle), F2 III, triple-system member, $v \sin i \sim 12$ km s^{-1}
  - 12 Com, HD 107700 (cross), G0 III-IV (SB), $v \sin i \sim 13$ km s^{-1}
  - 68 Peg, HD 220657 (open circle), F8 IV, $v \sin i \sim 60$ km s^{-1}
  - HD 77258 (filled circle), K0 III (SB)
  - 31 Com, HD 111812 (filled diamond), G0III, $v \sin i \sim 67$ km s^{-1}
  - 24 UMa, HD 82210 (filled triangle), G4 III-IV, $v \sin i \sim 10$ km s^{-1}

  Among the stars with $B-V > 0.8$ we observe a large range of X-ray emission levels ($27 < \log L_{\rm x} < 31$ erg s^{-1} and $2 < \log F_{\rm x} < 6$ erg cm^{-2} s^{-1}) apparently due to mixing of stars ascending the giant branch for the first time and clump giants.

- $M/M_{\odot} > 3.0$: these higher mass stars have $\log L_x < 29.5$ and $\log F_x \leq 4$, and appear to be mostly indistinguishable from the clump giants of lower mass.

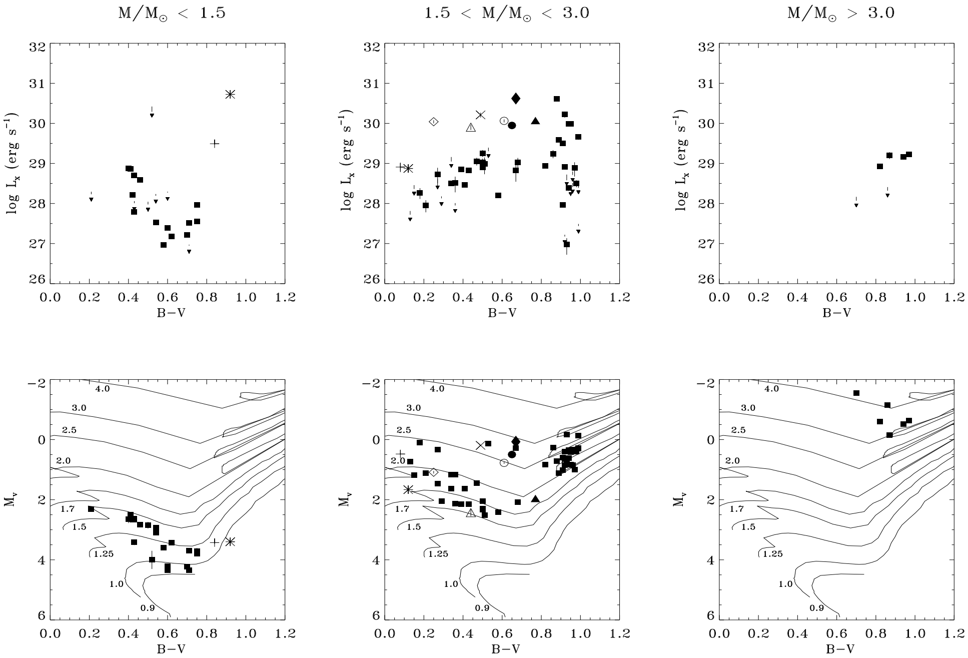

Figure 5. Distributions of X-ray luminosities (or upper limits) vs. B-V color for the stars in the ROSAT sample within 100 pc, in the three mass ranges indicated on top of each panel (top row). Selected X-ray sources with L_x higher than average are marked in color (see text for their identification). The panels in the bottom row show the corresponding distributions in the H-R diagram, where the Schaller et al. (1992) evolutionary tracks are also plotted.

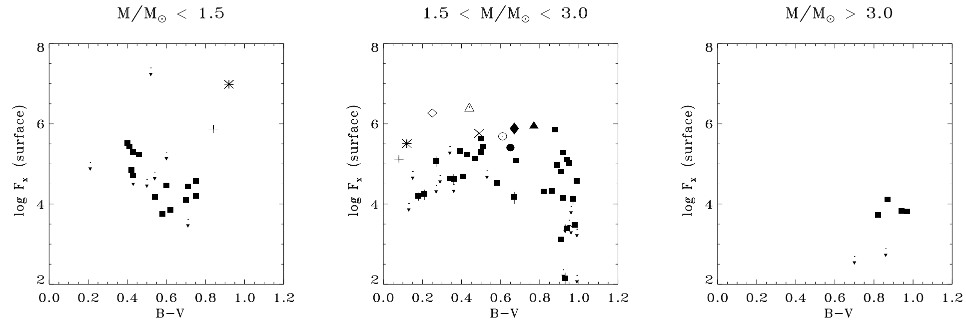

Figure 6. Distributions of surface X-ray fluxes (or upper limits) vs. B-V color for the stars in the ROSAT sample within 100 pc, in the three mass ranges indicated on top of each panel. The symbols in color are the same as in Fig. 5

The above scenario appears evident also from inspection of the L_x vs. B-V scatter plots derived from the *Einstein* and RIASS samples, shown in Fig. 7, where only the first two mass ranges were considered.

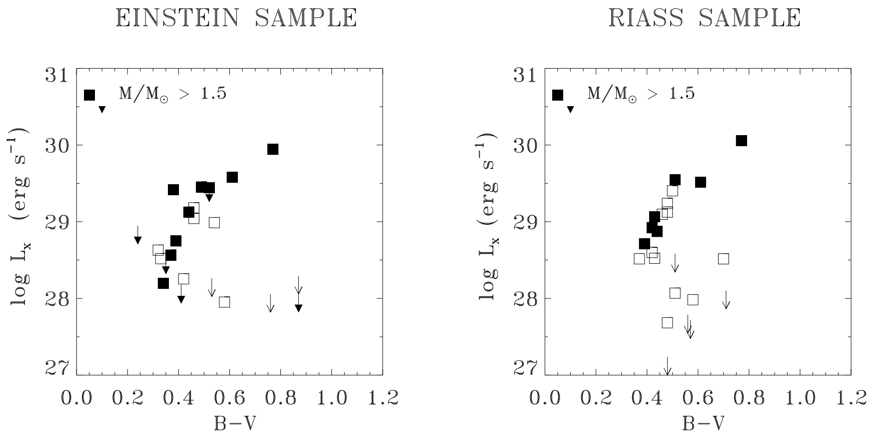

Figure 7. X-ray luminosity vs. B-V color for the stars in the *Einstein* and RIASS samples. Open and filled symbols are used for stars with $M/M_\odot < 1.5$ and $M/M_\odot > 1.5$, respectively.

4. Conclusions

Our study suggests the existence of a different evolutionary behavior of X-ray activity for stars with $M < 1.5 M_\odot$, which have spent most of their main-sequence life as X-ray emitters, with respect to stars with $1.5 < M/M_\odot < 3.0$ (A-type inactive stars on the main-sequence). In particular, there is a trend of increasing emission level with age for the intermediate mass stars, which is likely due to the influence of changes in stellar internal structure on magnetic dynamo efficiency. For stars with $B - V > 0.8$ we observe a large spread in L_x of about three orders of magnitude, possibly due to mixing of stars ascending the giant branch for the first time and clump giants. We plan to try discriminating these two classes of stars with a complementary study of CNO and Li abundances.

The above conclusions are in general agreement with the results based on previous works (see also Maggio et al. 1990; Hünsch & Schröder 1996), but emphasize the importance of studying the evolution of stellar X-ray activity using homogeneous star samples in selected mass ranges.

References

Ayres, T. R., Fleming, T. A., Simon, T. et al., 1995, ApJS, 96, 223

Barnes, T. G., Evans, D. S., Moffett, T. J. 1978, MNRAS, 183, 285

Damiani F., Maggio A., Micela G., Sciortino S. 1997, ApJ, 483, 350

Damiani F., Maggio A., Micela G., Sciortino S. 1997, ApJ, 483, 370

Duquennoy, A., Mayor, M. 1991, A&A, 248, 485

Mackie, G., Fabbiano, G., Harnden, F.R. et al. 1996, in Astronomical Data Analysis Software and Systems V, ASP Conf. Series 101, G.H. Jacoby and J. Barnes eds., 179

Maggio, A., Vaiana, G.S., Haisch, B. et al. 1990, ApJ, 348, 253

Maggio, A., Sciortino, S., Bianchi, L., Harnden, F.R., Jr., & Rosner, R. 1993, in Physics of Solar and Stellar Coronae, J. Linsky & S. Serio, Kluwer, 291

Hoffleit, D., & Warren, W.H., Jr. 1991, *The Bright Star Catalogue*, 5th Revised Ed. (Preliminary Version)

Hünsch, M., Schröder, K. P. 1996, A&A, 309, L51

Huebner, W. F., Merts, A. L., Magee, N. H., & Argo, M. F. 1977, Los Alamos Sci. Lab. Rept., LA-6760-M

Kurucz, R. L. 1979, ApJS, 40, 1

Kurucz, R. L. 1991, *Stellar Atmosphere-Beyond Classical Models*, p. 441

Rogers, F. J., Iglesias, C. A. 1992, ApJS, 79, 507

Schaller, G., Schaerer, D., Meynet, G., Maeder, A. 1992, A&AS, 96, 269

VandenBerg, D. A. 1985, ApJS, 58, 711